Are recent changes in sediment manganese sequestration in the euxinic basins of the Baltic Sea linked to the expansion of hypoxia?

C. Lenz[1,2], T. Jilbert[2], D.J. Conley[1], M. Wolthers[3,2] and C.P. Slomp[2]

[1]{ Department of Geology, Lund University, Sölvegatan 12, SE-22362 Lund, Sweden}

[2]{Department of Earth Sciences, Faculty of Geosciences, Utrecht University, Budapestlaan 4, 3584 CD Utrecht, the Netherlands}

[3]{University College London, Department of Chemistry, 20 Gordon Street, London, WC1H 0AJ, United Kingdom}

Correspondence to: C. Lenz (conny.lenz@geol.lu.se)

Abstract

Expanding hypoxia in the Baltic Sea over the past century has led to anoxic and sulfidic (euxinic) deep basins that are only periodically ventilated by inflows of oxygenated waters from the North Sea. In this study, we investigate the consequences of the expanding hypoxia for manganese (Mn) burial in the Baltic Sea using a combination of pore water and sediment analyses of well-dated sediment cores from 8 locations. Diffusive fluxes of dissolved Mn from sediments to overlying waters at oxic and hypoxic sites are in line with an active release of Mn from these areas. However, this flux of Mn is only small when compared to the large pool of Mn already present in the hypoxic and anoxic water column. Our results highlight two modes of Mn carbonate formation in sediments of the deep basins. In the Gotland Deep area, Mn carbonates likely form from Mn oxides that are precipitated from the water column directly following North Sea inflows. In the Landsort Deep, in contrast, Mn carbonate and Mn sulfide layers form independent of inflow events, with pore water Mn produced in deeper layers of the sediment acting as a key Mn source. While formation of Mn enrichments in the Landsort Deep continues to the present, this does not hold for the Gotland Deep area. Here, increased euxinia, as evident from measured bottom water sulfide concentrations and elevated sediment molybdenum (Mo), goes hand in hand with a decline in sediment Mn and recent

inflows of oxygenated water (since ca. 1995) are no longer consistently recorded as Mn carbonate layers. We postulate that, because of the quicker return of high sulfide concentrations in the water column, the reduction of Mn oxides following an inflow has become so rapid that the Mn^{2+} is released to the water column before Mn carbonates can form. Our results have important implications for the use of Mn carbonate enrichments as a redox proxy in marine systems.

1 Introduction

Manganese (Mn) enrichments in sedimentary deposits are often used as an indicator of redox changes in the overlying waters (e.g. Calvert and Pedersen, 1993). In anoxic settings, Mn-enrichments are typically assumed to consist of Mn carbonates, which are associated with calcium and can contain other impurities (e.g. Jakobsen and Postma, 1989; Manheim, 1961; Sternbeck and Sohlenius, 1997; Suess, 1979). These minerals are suggested to form from Mn oxides deposited during a period of bottom water oxygenation (Calvert and Pedersen, 1996; Huckriede and Meischner, 1996), with Mn^{2+} availability thought to be the key control (Neumann et al., 2002). However, sediment Mn data for both the Landsort Deep in the Baltic Sea (Lepland and Stevens, 1998) and the Black Sea (Lyons and Severmann, 2006) indicate that Mn enrichments may also form in sediments overlain by continuously anoxic bottom waters. In the Landsort Deep, these enrichments consist of both Mn carbonates and Mn sulfides (Lepland and Stevens, 1998; Suess, 1979). The formation of both mineral phases is assumed to be driven by an exceptionally high alkalinity, with Mn sulfides forming when H_2S exceeds Fe availability (Böttcher and Huckriede, 1997; Lepland and Stevens, 1998). Finally, Mn enrichments may also form in sediments overlain by oxic bottom waters upon increased input and precipitation of Mn oxides and transformation to Mn carbonate during burial (e.g. MacDonald and Gobeil, 2012; Mercone et al., 2001). A better understanding of the various modes of formation of sedimentary Mn and the link with variations in bottom water redox conditions is essential when interpreting Mn enrichments in geological deposits (e.g. Calvert and Pedersen, 1996; Huckriede and Meischner, 1996; Jones et al., 2011; Meister et al., 2009).

The Baltic Sea provides an ideal environment for studies of redox-dependent Mn dynamics because of the large spatial and temporal variations in oxygen conditions over the past century, that are especially well documented since the 1970's (Fonselius and Valderrama, 2003). Besides providing evidence for sporadic inflows of oxygenated saline water from the

North Sea that affect brackish bottom waters in all deep basins, the available hydrographic data indicate a major expansion of the hypoxic area in the Baltic Sea linked to increased eutrophication (Carstensen et al., 2014; Conley et al., 2009; Gustafsson et al., 2012; Savchuk et al., 2008). While the shallower areas in the Baltic Sea are now seasonally hypoxic, the deep basins all show a major shift towards anoxic and sulfidic (euxinic) conditions around 1980 (Fonselius and Valderrama, 2003; Mort et al., 2010). These basin-wide changes in redox conditions likely had a major impact on both the sources and sinks of sediment Mn in the Baltic Sea.

River input (Ahl, 1977; Martin and Meybeck, 1979) and release from sediments (Sundby et al., 1981; Yeats et al., 1979) are the key sources of Mn in the water column of marine coastal basins. While in areas with oxic bottom waters, dissolved Mn produced in the sediment will mostly be oxidized to Mn oxide in the surface layer and thus will be trapped in the sediment, dissolved Mn may escape to the overlying water when the oxic surface layer is very thin (Slomp et al., 1997). In the water column, this Mn may be oxidized again (e.g. Dellwig et al., 2010; Turnewitsch and Pohl, 2010) and contribute to the depositional flux of Mn oxides, or may be laterally transferred in dissolved or particulate form. The lateral transfer of Mn from oxic shelves to deep basins, where the Mn may be trapped and ultimately may precipitate as an authigenic mineral, is termed the "Mn shuttle" (Lyons and Severmann, 2006).

In a basin with expanding hypoxia and anoxia, as is the case in the Baltic Sea over the past century (Conley et al., 2009), the Mn shuttle is expected to have become more efficient in transporting Mn to deeper, euxinic basins because of decreased trapping of Mn in oxygenated surface sediments (Lyons and Severmann, 2006). We postulate that, during the first phase of the expansion of bottom water hypoxia, there may even have been a "pulse" of release of Mn from the sediments. During an extended period of hypoxia and anoxia, however, sediments in hypoxic areas may become depleted of Mn oxides, thus reducing the strength of the Mn shuttle. In addition, the formation rate of authigenic Mn minerals at deep basin sites may change in response to hypoxia and anoxia. If dissolved Mn^{2+} is the dominant control for Mn carbonate formation as suggested for the Gotland Deep (Neumann et al., 2002), expanding anoxia could allow Mn oxides to be reduced in the water column and at the sediment-water interface, precluding conversion to Mn carbonates. This mechanism was recently invoked to explain the lack of Mn carbonates during periods of bottom water euxinia in the Gotland Deep during the Holocene Thermal Maximum (Lenz et al., 2014). If alkalinity is the key

control, however, as suggested for the Landsort Deep (Lepland and Stevens, 1998), Mn sequestration could be similar or increase due to higher rates of sulfate reduction.

In this study, we use geochemical analyses of well-dated sediment cores for 8 sites in the Baltic Sea, combined with pore water data to assess the role of variations in water column redox conditions for Mn dynamics in the Baltic Sea. We capture the full range of redox conditions (oxic, hypoxic and euxinic) to investigate the cycling of Mn in the sediment, the present-day diffusive flux from the sediments and the sequestration of Mn in mineral phases. While the pore water data only provide a "snapshot" of the conditions at the time of sampling, the sediment data in the euxinic basins record both the expansion of hypoxia and anoxia and the effects of short-term inflows of oxygenated water. Our results indicate release of Mn from oxic and hypoxic areas as well as the deep basin sites, and sequestration of Mn carbonates and sulfides in the Landsort Deep. The lack of recent Mn accumulation in many deep basin sites suggests that inflows of oxygenated seawater are no longer recorded by Mn carbonate deposits.

2 Materials and Methods

2.1 Study area

Sediments from 8 locations in the southern and central Baltic Sea were collected during 4 cruises between 2007 and 2011 (Figure 1, Table 1) using a multi-corer. The sites differ with respect to their water depths and their present-day bottom water redox conditions. The Fladen and LF1 sites are located in the Kattegat and along the eastern side of the Gotland Deep, respectively, and are fully oxic, whereas site BY5 in the Bornholm Basin is seasonally hypoxic (Jilbert et al., 2011; Mort et al., 2010). The remaining stations, LF3, LL19, BY15, F80 and LD1, are situated below the redoxcline, which was located between 80 and 120 m water depth at the time of sampling. Therefore, these sites are all currently anoxic and sulfidic (euxinic). The latter 4 sites are located in the deep central basins of the Baltic Sea, at water depths ranging from 169 m at LL19 to 416 m at LD1 (Baltic Sea Environmental Database at Stockholm University; http://nest.su.se/bed/ACKNOWLE.shtml).

2.2 Bottom water and pore water analyses

At each site, sediment multi-cores (<50 cm, 10 cm i.d.) were either immediately sectioned in a N_2-filled glovebox at in-situ temperature or sampled with syringes through pre-drilled holes

in the core liner. A small portion of each sample was stored at 5°C or -20°C in gas-tight jars for sediment analyses. The remaining sediment was centrifuged (10-30 min.; 2500 g) in 50 ml greiner tubes to collect pore water. Both the pore water and a bottom water sample were filtered (0.45 μm pore size) and subdivided for later laboratory analyses. All pore water handling prior to storage was performed in a N_2 atmosphere. A subsample of 0.5 ml was directly transferred to a vial with 2 ml of a 2% Zn-acetate solution for analysis of hydrogen sulfide. Sulfide concentrations were determined by complexation of the ZnS precipitate using phenylenediamine and ferric chloride (Strickland and Parsons, 1972). Subsamples for total Mn and S were acidified with either HNO_3 (Fladen, BY5) or HCl (all other stations) and stored at 5°C until further analysis with ICP-OES (Perkin Elmer Optima 3000; relative precision (<5%) and accuracy were established by standards (ISE-921) and duplicates). Hydrogen sulfide was assumed to be released during the initial acidification, thus S is assumed to represent SO_4^{2-} only. Total Mn is assumed to represent Mn^{2+}, although some Mn^{3+} may also be included (Madison et al., 2011). Subsamples for NH_4 were frozen at -20°C until spectrophotometric analysis using the phenol hypochlorite method (Riley, 1953). A final subsample was used to determine the pH with a pH electrode and meter (Sentron). Note that degassing may impact ex-situ pH measurements and may lead to a rise in pH (Cai and Reimers, 1993). The total alkalinity was then titrated with 0.01 M HCl. All colorimetric analyses were performed with a Shimadzu spectrophotometer. Replicate analyses indicated that the relative error for the pore water analyses was generally <10 %.

2.3 Sediment analyses

Sediment samples were freeze-dried and water contents were calculated from the weight loss. Sediments were then ground in an agate mortar in a N_2 or argon-filled glovebox. From each sediment sample, aliquots for several different analyses were taken. For total organic carbon (TOC) analyses, 0.3 mg of sediment was decalcified with 1M HCl and the C content was determined with a Fisons NA 1500NCS. Based on laboratory reference materials and replicates, the relative error for organic C was generally less than 5%. Total sediment contents of S, Mn and Mo were determined with ICP-OES, after dissolution of 0.125 mg of sample with an $HF/HClO_4/HNO_3$ mixture in closed Teflon bombs at 90°C, followed by evaporation of the solution and redissolution of the remaining gel in 1M HNO_3. The accuracy and precision of the measurements were established by measuring laboratory reference materials

(ISE-921 and in-house standards) and sample replicates; relative errors were <5% for all reported elements.

Age models based on ^{210}Pb analyses for 6 multi-cores used in this study have been previously published. For details, we refer to the relevant papers: Fladen and BY5 (Mort et al., 2010), LF1 and LF3 (Jilbert et al., 2011), LL19 (Zillén et al., 2012) and BY15 (Jilbert and Slomp, 2013). A new ^{210}Pb age model was constructed for LD1. Samples from LD1 were analyzed with a Canberra BeGe gamma ray spectrometer at Utrecht University. The samples were freeze-dried, homogenized, and transferred into vent-free petri dishes, which were sealed in polyethylene bags and stored for 2 weeks before measuring. Each sample was measured until 200-250 ^{210}Pb gamma-ray counts were reached. For the age determination a constant rate of supply model (Appleby and Oldfield, 1983) was implemented using a background estimated from the mean counts of ^{214}Pb and ^{214}Bi. For further details on the age models and the ^{210}Pb data for LD1, we refer to the supplementary information Appendix A. The age model for F80 was constructed using high resolution Mo and Mn data. In 2013, an extra sediment core from this station was taken and mini sub-cores as described in section 2.4 were embedded in Spurr´s epoxy resin and measured by LA-ICP-MS. The fluctuations in Mo/Al and Mn/Al ratios were coupled to the instrumental records of bottom water oxygen conditions. The 2009 multicore profiles were subsequently tuned to the dated profiles from 2013 (see Appendix A for more details).

2.4 Microanalysis

Mini sub-cores of 1 cm diameter and up to ~12 cm length each were taken from the top part of sediment multicores at sites LL19 and LD1 in May 2011 as described by Jilbert and Slomp (2013). Briefly, the pore water was replaced by acetone and the sub-core was fixed in Spurr´s epoxy resin. During the whole procedure the sub-cores remained upright. During the dewatering process the sediment compacted resulting in a reduction of length of both sections by up to 50%. After curing, epoxy-embedded sub-cores were opened perpendicular to the plane of sedimentation and the exposed internal surface was polished.

Line scans were performed with LA-ICP-MS, to measure high-resolution vertical profiles of selected elements in the resin blocks of the two cores. A Lambda Physik laser of wavelength 193 nm and pulse rate of 10 Hz was focused onto the sample surface with a spot size of 120 µm. During line scanning, the sample was moved under the laser beam with a velocity of

0.0275 mm/s, creating an overlapping series of pulse craters. From the closed sample chamber the ablated sample was transferred to a Micromass Platform ICP-MS by He-Ar carrier gas. Specific isotopes of aluminum (^{27}Al), iron (^{57}Fe), manganese (^{55}Mn), sulfur (^{34}S) and molybdenum (^{98}Mo) were measured. For site LD1, bromine (^{81}Br) was also measured. LA-ICP-MS data for each element were calibrated by reference to the sensitivities (counts/ppm) of the glass standard NIST SRM 610 (Jochum et al., 2011) and corrected for the natural abundances of the analyzed isotopes. All data are reported normalized to Al to correct for variations in sample yield. For S/Al data, a further sensitivity factor was applied which compensates for the contrasting relative yield of S from NIST SRM 610 with respect to embedded sediments.

The resin-embedded samples were also mounted inside an EDAX Orbis Micro XRF Analyzer to construct elemental maps at a spatial resolution of 30 µm for manganese (Mn), calcium (Ca) and sulfur (S) (Micro XRF settings: Rh tube at 30 kV, 500 µA, 300 ms dwell time, 30 µm capillary beam).

To allow comparison of the data from the micro analyses with the discrete samples, the measured profiles of the LA-ICP-MS were extended to the original length of the core section and aligned to the samples data for the same depth interval (not shown).

2.5 Flux calculations

The diffusive flux of manganese across the sediment-water interface (J_{sed}) was calculated from the concentration gradient in the pore water over the upper 0.25 to 2.5 cm of the sediment with Fick's first law:

$$J_{sed} = -\varphi * D_{sed} * (\delta C/\delta x)$$

where φ is the porosity, D_{sed} is the whole sediment diffusion coefficient, C is the Mn concentration and x is depth in the sediment. D_{sed} was calculated from the diffusion coefficient in free solution corrected for salinity and temperature (D^{SW}) and porosity (Boudreau, 1997):

$$D_{sed} = D^{SW} / 1 - \ln(\varphi^2)$$

Whenever possible (LF3, LL19, BY15 and F80) higher resolution data from the 2009 Aranda cruise was used for the calculation (table 2 and data in Appendix B).

2.6 Saturation state

Thermodynamic equilibrium calculations have been performed for the pore water of LF3, LL19, BY15, F80 and LD1 using version 3.1.1 of the computer program PHREEQC (Parkhurst and Appelo, 1999) with the LLNL database. The database does not contain the authigenic carbonate phase present in the Baltic Sea. Data from the literature (Jakobsen and Postma, 1989; Sternbeck and Sohlenius, 1997; Lepland and Stevens, 1998; Huckriede and Meischner 1996; Kulik et al., 2000) suggests that carbonates mainly consist of Mn and Ca. Therefore, an approximation of the solubility product of (Mn, Ca) CO_3 solid solutions was generated using the equations given in Katsikopoulos et al. (2009). The stoichiometric solubility product (K_{st}) was calculated using $Mn_{0.74}Ca_{0.26}CO_3$ (Kulik et al 2000) as a common ratio measured for (Mn, Ca) CO_3 solid solutions in Baltic Sea sediments.

An equilibrium constant pK of 0.377 (Emerson et al. 1983) was used for Mn sulfide. The solubility of iron sulfide from Rickard (2006) was added to the calculations as well as $MnHS^+$ as a solute (Luther et al., 1996) because it is likely abundant in pore water in sulfidic sediments (Heiser et al., 2001). Carbonate alkalinity was calculated from titration alkalinity as described by Carman and Rahm (1997).

3 Results

At the time of sampling, bottom waters were oxic at the Fladen and LF1 sites, hypoxic at the Bornholm Basin site BY5, and anoxic and sulfidic at all other locations (Table 1). Pore water Mn^{2+} concentrations increase with depth in the sediment at most sites (Figure 2). At the Fladen site, however, Mn^{2+} concentrations decrease again below ca. 5 cm and at sites LF1 and LF3, Mn^{2+} is nearly absent. Alkalinity and ammonium concentrations increase with sediment depth, with the increase going hand in hand with a decline in sulfate. Sulfate concentrations in the bottom water at the different stations are in line with the salinity gradient in the Baltic Sea (Table 1). Concentrations of hydrogen sulfide in the pore water > 2 mM are found at the Fårö

Deep and Landsort Deep sites F80 and LD1. Saturation indices for $MnCaCO_3$ are positive below the surface sediment at the Landsort Deep, indicating supersaturation of the pore water with respect to this mineral. The other hypoxic and anoxic sites except LF3 reach saturation only at greater depth. For Mn sulfide, in contrast, supersaturation is only observed at the Landsort Deep site, LD1 (Figure 3) and below 35 cm at site F80. Calculated diffusive fluxes of Mn^{2+} vary over a wide range, with the highest efflux from the sediment being observed at the hypoxic Bornholm Basin site BY5 and in the anoxic Landsort Deep (LD1)(Table 2).

Average sedimentation rates vary significantly between sites, with 3- to 4-fold higher rates at Fladen and in the Landsort Deep when compared to LF1 and BY5 (Table 1; Figure 4). Sediments are rich in organic carbon (TOC) with maxima of ca. 5 wt% at the oxic sites Fladen and LF1 and ca. 16 wt% at the anoxic sites (Figure 4). While changes in TOC with depth at Fladen and LF1 are relatively small, distinct enrichments in TOC are observed in the upper part of the sediment at all anoxic sites. Total sulfur contents are low at Fladen, but are higher at all other sites, and show considerable variation with depth in the sediment. Mn is enriched in the surface sediment at Fladen, but is nearly absent at the LF1, BY5 and LF3 sites. At sites LL19, BY15, F80 and LD1, Mn is present again but is mostly observed at greater depth in the sediment. Sediment Mo is low at the Fladen, LF1, BY5 and LF3 sites but is enriched at the other sites, where profiles largely follow those of TOC.

The LA-ICP-MS line-scans of resin-embedded surface sediments at site LL19 (Figure 5A) support the results of the discrete sample analysis (Figure 4) and confirm that there are very few Mn rich laminae in recent sediments at this location. While most of the minor enrichments of Mn are correlated with Fe, S and Mo (Figure 5A), three peaks (at 3.6, 3.9 and 4.6 cm) are independent of these elements, suggesting that these Mn enrichments dominantly consist of carbonates. This is confirmed by the Micro-XRF maps (Figure 5B) of the corresponding interval, which indicate coincident Mn and Ca-rich layers. The maps show clear Mn carbonate layers at ~3.9 cm and ~4.6 cm. However, the third enrichment at 3.6 cm is less continuous and is only represented by one spot in the map. The two distinct Mn-carbonate layers can be linked to inflow events in 1993 and 1997, using the ^{210}Pb-based age model for this site, after correction for compaction of the sediment during embedding.

In the surface sediments of station LD1, in contrast, a large number of Mn enrichments with much higher concentrations than at LL19 are observed (Figure 4 and 5). The LA-ICP-MS line scans show that highest values often coincide with enrichments in S, Mo and Br but are not

related to maxima in Fe. The micro-XRF-maps of Mn, Ca and S confirm that enrichments in Mn are present as discrete layers. The RGB (Mn, Ca, S) composite reveals two different compositions for the Mn enrichments. The purple layers in the RGD composite are a result of enrichments of Mn (red) and S (blue) in the same pixel, suggesting the presence of Mn sulfide. However, other layers and spots are orange to yellow, indicating coincident enrichments of Ca (green) and Mn, suggesting carbonate enrichments (Figure 5B).

4 Discussion

4.1 Sediment Mn cycling in the Baltic Sea

Our results indicate major differences in Mn dynamics in the varied depositional settings of the Baltic Sea. Although located in the Kattegat far from the euxinic basins, processes at the Fladen site (Fig. 2 and 3) can be used to illustrate the typical processes at oxic sites. Here, Mn cycling is largely internal to the sediment and the Mn that is released to the pore water at depth mostly reprecipitates upon upward diffusion into the oxic surface sediment. At the hypoxic site in the Bornholm Basin (BY5) there is no clear sediment Mn enrichment but there is release of dissolved Mn to the pore water, presumably due to dissolution of Mn oxides, within the upper 15 cm of the sediment. At this site, the highest diffusive Mn flux from the sediment to the water column was found (Table 2). At the sites on the slope of the eastern Gotland Basin (LF1 and LF3), in contrast, the sediments are nearly completely devoid of Mn, both in the pore water and solid phase. This highlights that while sediments in some hypoxic areas, such as the Bornholm Basin, may still act as sources of Mn to the water column, with subsequent lateral transfer potentially bringing this Mn to the deep basins (Huckriede and Meischner, 1996; Jilbert and Slomp, 2013; Lyons and Severmann, 2006; Scholz et al., 2013), sediments in some shallow areas no longer do so.

The pore water profiles of the 4 anoxic sites in the various deep basins (LL19, BY15, F80, and LD1) all are indicative of release of Mn to the pore water, either from dissolution of Mn oxides or Mn carbonates (e.g. Heiser et al., 2001; Jilbert and Slomp, 2013). As a result, diffusive Mn fluxes are also observed at all these deep basin sites. However, the Mn released to these deep waters remains trapped below the redoxcline in the water column. Although reoxidation of the Mn and formation of mixed phases of Mn oxides and Fe-(III)-associated phosphates upon upward diffusion of Mn into the redoxcline occurs (Dellwig et al., 2010;

Turnewitsch and Pohl, 2010), sinking of these phases into sulfidic waters leads to subsequent reductive redissolution.

Due to the seasonal and inflow-related changes in redox conditions in the Baltic Sea and our very limited number of study sites, we cannot accurately estimate the importance of the present-day source of Mn from oxic and hypoxic areas at the basin scale. However, we do note that the range in Mn fluxes in our study (0 to 236 μmol m^{-2} d^{-1}; Table 2) is comparable to benthic fluxes measured with in-situ chambers in other areas of the Baltic Sea (e.g. the Gulf of Finland; Pakhomova et al., 2007) and estimated from pore water profiles from the 1990's (e.g. Heiser et al., 2001). As discussed by Heiser et al. (2001), an efflux of Mn of this order of magnitude is relatively small compared to the total amount of dissolved Mn in the hypoxic water, which these authors estimate at 0.8 mol MnO_2 m^{-2} for an anoxic water column of 100 m in the Gotland Basin. This large pool of Mn in the water column was likely mostly released from the formerly oxic sediments during the initial expansion of hypoxia during the 20th century, and is now only temporarily precipitated again as Mn oxide when the basin becomes oxygenated during inflows (Yakushev et al., 2011). Thus, in contrast to the period of initial expansion of hypoxia, the Mn pool in the water column now depends largely on ambient redox conditions. This is supported by the fact that there is no trend in water column Mn concentrations with time over recent decades (Pohl and Hennings, 2005). We conclude that the present-day Mn shuttle, although active in transporting Mn from the shallow to deep areas, is not as important quantitatively as a source of Mn to the deep basins as it was at the onset of hypoxia early in the 20th century.

4.2 Manganese sequestration in the anoxic basins

Formation of Mn bearing carbonates in the Gotland Basin and Landsort Deep is generally described as being ubiquitous (e.g. Jakobsen and Postma, 1989). When bottom waters in the deep basins of the Baltic Sea are anoxic, pore waters in the surface sediments are typically undersaturated with respect to Mn(Ca) carbonates down to a depth of ~5 to 8 cm (Figure 3)(Carman and Rahm, 1997; Heiser et al., 2001). However, strong oversaturation is assumed to be reached following the inflow of oxygenated, saline North Sea water (Huckriede and Meischner, 1996; Sternbeck and Sohlenius, 1997). Various authors have correlated such inflow events to specific accumulations of Mn carbonate in sediments of the Gotland Basin (e.g. Heiser et al., 2001; Neumann et al., 1997). We observe such enrichments in all our deep basin cores, with the magnitude of the enrichment increasing with water depth (Fig. 4).

Increased focusing of Mn oxides with water depth has been observed in other marine systems (e.g. Slomp et al., 1997) and high alkalinity in sulfate-bearing organic rich sediments overlain by an anoxic water column are typically linked to organic matter degradation through sulfate reduction (Berner et al., 1970).

Our microanalysis results show that the Mn carbonate enrichments at site LL19 are highly laminar in character, implying rapid precipitation at the sediment-water interface. Furthermore, these Mn carbonate enrichments occur independently of enrichments in Mo and S, suggesting relatively oxic conditions at the time of precipitation. Both lines of evidence support the interpretation of Mn carbonate precipitation within a very short time, possibly only weeks, following inflow events (Sternbeck and Sohlenius, 1997). Our age model suggests that the two pronounced Mn carbonate layers at the base of the surface-sediment block (Fig. 5) correspond to inflows in 1993 and 1997 (Matthäus and Schinke, 1999).

Mn enrichments at the Landsort Deep site LD1 occur more frequently when compared to other deep basin sites (Figure 4), as observed in earlier work (Lepland and Stevens, 1998). In the Landsort Deep, Lepland and Stevens (1998) attributed the enrichments to the relatively high alkalinity. Our pore water results show that the alkalinity is similar to that of F80. However, the pore water Mn^{2+} concentrations at the Landsort Deep site are much higher than elsewhere. This suggests that dissolution of Mn minerals below the surface sediment supplies additional Mn for Mn carbonate formation in the Landsort Deep and allows the more continuous formation. While such a deep sediment pore water source of Mn^{2+} is also observed at the other sites (e.g. LL19 and F80), and may be linked to dissolution of Mn carbonates at greater depth (Heiser et al., 2001; Jilbert and Slomp, 2013), the pore water Mn concentrations are by far the highest at the Landsort Deep site (> 1 mM versus <0.26 mM of Mn^{2+}). This "deep" source of Mn may in fact explain why the formation of Mn enrichments is more continuous than at the other sites, rather than the difference in alkalinity as suggested earlier by Lepland and Stevens (1998). We note that the Landsort Deep is the deepest basin in the Baltic Sea and its geometry makes it an excellent sediment trap. As a consequence, sediment deposition rates are much higher than in the other Deeps (Expedition 347 Scientists, 2014; Lepland and Stevens, 1998; Mort et al., 2010), explaining the observed differences in pore water chemistry.

The high-resolution analyses for the Landsort Deep site (LD1) also show that, besides Mn carbonate enrichments, there are several distinct layers of Mn sulfide in the surface sediments

(Fig. 5). These appear to coincide with enrichments in Mo, suggesting formation of Mn sulfides during intervals of more reducing conditions (Mort et al., 2010). Furthermore, we observe simultaneous enrichments of Br (Fig. 5), which suggests higher organic carbon contents (Ziegler et al., 2008). These results could imply that increased rates of sulfate reduction linked to elevated inputs of organic material to the sediments drive the formation of Mn sulfide. We note that the interval presented in the XRF map covers only a few years of sediment accumulation, possibly suggesting rapid changes in Mn mineralogy in response to seasonal variability of the organic matter flux (Fig. 5). Primary productivity in the Baltic Sea is known to vary seasonally (Bianchi et al., 2002; Fennel, 1995). Further work is required to determine conclusively the mechanisms of the MnS formation. While the presence of MnS has been shown for the earlier anoxic time intervals in the Baltic (Böttcher and Huckriede, 1997; Lepland and Stevens, 1998), this is the first time Mn sulfides are reported for such near-surface sediments in the Baltic Sea.

The contrasting controls on Mn mineral formation in the Landsort Deep, compared to the other deep basin sites, are further illustrated by a comparison of the trends in total Mn and Mo concentrations (Figure 4) with measured bottom water oxygen concentrations for the period 1955 to 2010 (Baltic Sea Environmental Database in Gustafsson and Medina (2011)) for sites in the northern Gotland Basin (LL19) and the Landsort Deep (LD1) (Figure 6). At site LL19, Mn enrichments in the sediments coincide with low values of Mo in the sediment and inflows of oxygenated water. At LD1, in contrast, high Mn contents are observed from 1965 onwards, independent of inflows, with the highest Mn values coinciding with the most euxinic periods, which mostly occurred after the year 2000.

4.3 Changes in Mn burial linked to expanding hypoxia

Strikingly, the more reducing conditions in the Gotland Basin (LL19, BY15) and Fårö Deep sites (F80) over the past decades, as recorded in the Mo profiles (Figures 4 and 6), are accompanied by a strong reduction in sediment Mn burial. Given the suggested link between Mn burial and inflows, it is important to assess their occurrence. During the past two decades, there were two major (1993, 2003) and several minor inflow events (e.g. 1997) into the Baltic Sea. The event in 1993 was one of the strongest in the last 60 years (Matthäus et al., 2008) and the inflow of 2003 (Feistel et al., 2003) was weaker but still significant enough to reoxygenate the bottom water of the deep basins (Figure 6). However, at LL19, Mn sequestration in the sediment between 2000 and 2010 has been negligible and the inflow in

2003 is not recorded as a Mn carbonate enrichment (Figure 6), whereas in the high resolution geochemical analyses Mn layers are clearly visible in both the LA-ICP-MS and micro-XRF scans (Figure 5) and can be linked to the inflows in 1993 and 1997. A similar "missing" Mn carbonate layer was observed by Heiser et al. (2001) in the Gotland Deep and attributed to re-dissolution of Mn carbonate linked to resuspension events and mixing of the sediment into unsaturated bottom waters. However, our cores were clearly laminated and the ^{210}Pb profiles also show no evidence for mixing. We therefore conclude that, with the increased hypoxia and euxinia in the Baltic Sea, Mn oxides are no longer converted to stable Mn carbonates following inflows.

The formation of Mn carbonates in Baltic Sea sediments is typically believed to be induced by the high alkalinity linked to organic matter degradation combined with high Mn^{2+} concentrations in the surface sediment upon dissolution of Mn oxides following inflows (Lepland and Stevens, 1998). But what can inhibit the formation of these Mn carbonates? One possibility is that at high pore water sulfide concentrations, Mn sulfides form instead of Mn carbonates. However, given that there is negligible Mn enrichment in the upper sediments of F80, BY15 and LL19 today, we can exclude that possibility. Mn carbonate formation could be reduced if alkalinity declined, but alkalinity in the bottom waters of the Gotland Deep has in fact increased recently (e.g. Ulfsbo et al., 2011). High phosphate concentrations in the surface sediment may potentially negatively affect the rate of Mn carbonate formation (Mucci, 2004). However, there is no evidence for a significant rise in dissolved phosphate in the pore water of Gotland Basin sediments over the past decades (e.g. Carman and Rahm, 1997; Hille et al., 2005; Jilbert et al., 2011). We postulate that Mn oxides that are formed following modern inflow events are dissolved much faster than previously because of the more rapid return of sulfide in the surface sediments and the higher sulfide concentrations in the water column linked to the expansion of hypoxia. As a consequence, the Mn^{2+} released from the oxides escapes to the overlying water instead of being precipitated in the form of Mn carbonate. In the Fårö and Gotland Deep sediments, recent Mo enrichments go hand in hand with Mn depletions and permanent euxinia in bottom waters (Figure 6). Given that sinking Mn oxides particles do not survive downward transport through a sulfidic water column (Dellwig et al., 2010), these results further imply that sinking Mn oxides are, at present, likely not the main carrier of Mo to the sediment in the Baltic Sea. This observation suggests that, contrary to suggestions by Scholz et al. (2013), scavenging of Mo by Mn (oxyhydr)oxides is not at present a major vector for Mo delivery to the sediment surface in the Gotland Deep.

4.4 Implications for Mn as a redox proxy

In the classic model of Calvert and Pedersen (1993), Mn enrichments in sediments are indicative of either permanent or temporary oxygenation of bottom waters. Sediments of permanently anoxic basins, in contrast, are assumed to have no authigenic Mn enrichments because there is no effective mechanism to concentrate the Mn oxides. Our results for the Gotland Deep area indicate that the temporary oxygenation of the basin linked to inflows is no longer recorded as a Mn enrichment in the recent sediment when hypoxia becomes basin-wide. Thus, a decline in Mn burial (or a complete lack of Mn) in geological deposits in combination with indicators for water column euxinia such as elevated Mo contents may point towards expanding hypoxia, but does not exclude temporary oxygenation events. Strikingly, only very little Mn was buried at sites F80 and LL19 during the previous period of hypoxia in the Baltic Sea during the Medieval Climate Anomaly (Jilbert and Slomp, 2013) as well as at the end of the Holocene Thermal Maximum at site LL19 (Lenz et al., 2014). This may be in line with hypoxia that was equally intense and widespread in the basin at the time as it is today. Our results for the Landsort Deep indicate that Mn enrichments may also form frequently in an anoxic basin as Mn carbonates and sulfides if there is a deep pore water source of dissolved Mn^{2+}. Such a deep source is expected to be important at sites where abundant Mn has accumulated during previous periods of more oxic conditions. Mn enrichments in geological deposits thus can be indicative of both oxic and anoxic depositional environments, emphasizing the need for multiple redox proxies.

5 Conclusions

Our work demonstrates that the efflux of Mn from sediments in the Baltic Sea is relatively small compared to the existing reservoir of Mn in the anoxic deep waters. Although abundant dissolved Mn is available in the water column, Mn-enrichments are no longer forming in all of the anoxic basins of the central Baltic Sea. We show that the most recent sediments in the Fårö Deep and Gotland Deep contain low concentrations of Mn near the sediment surface. We postulate that this is due to the expansion of hypoxia over the past decades with the Mn oxides formed during inflows from the North Sea often being reduced so rapidly that the Mn^{2+} is lost to the water column. In Landsort Deep, in contrast, Mn sulfides and carbonates are still being precipitated. This is attributed to an additional diffusional source of Mn from deeper pore water. Our results indicate that sediment Mn carbonates in the Baltic Sea no longer

reliably record inflows of oxygenated North Sea water. This has implications for the use of Mn enrichments as a redox proxy when analyzing geological deposits.

Acknowledgements

This work was funded by grants from the Baltic Sea 2020 foundation, the Netherlands Organisation for Scientific Research (Vidi-NWO), Utrecht University (via UU short stay fellowship 2011), the EU-BONUS project HYPER and the European Research Council under the European Community's Seventh Framework Programme for ERC Starting Grant #278364. MW acknowledges Natural Environment Research Council [fellowship #NE/J018856/1]. We thank the captain and crew of RV Skagerrak (2007), RV Aranda (2009), RV Heincke (2010) and RV Pelagia (2011) and all participants of the cruises for their assistance with the field work. We thank Simon Veldhuijzen for his contribution to the analyses for site F80. Bo Gustafsson is thanked for providing water column data.

References

Ahl, T.: River Discharges of Fe, Mn, Cu, Zn, and Pb into the Baltic Sea from Sweden, Ambio Special Report, 219-228, 1977.

Appleby, P. and Oldfield, F.: The assessment of ^{210}Pb data from sites with varying sediment accumulation rates, Hydrobiology, 103, 29-35, 1983.

Berner, R. A., Scott, M. R. and Thomlinson, C.: Carbonate alkalinity in the pore waters of anoxic marine sediments, Limno. Oceanogr. 15(4), 544-549, 1970.

Bianchi, T. S., Rolff, C., Widbom, B., and Elmgren, R.: Phytoplankton Pigments in Baltic Sea Seston and Sediments: Seasonal Variability, Fluxes, and Transformations, Estuar Coast Shelf Sci, 55, 369-383, 2002

Böttcher, M. E. and Huckriede, H.: First occurrence and stable isotope composition of authigenic γ-MnS in the central Gotland Deep (Baltic Sea), Mar Geol, 137, 201-205, 1997.

Boudreau, B. P.: Diagenetic models and their implementation: modelling transport and reactions in aquatic sediments, Springer Berlin, 1997.

Cai, W.-J and Reiners, C. E.: The development of pH and pCO_2 microelectrodes for studying the carbonate chemistry of pore waters near the sediment-water interface, Limnol. Oceanogr., 38(8), 1762-1773, 1993.

Calvert, S. and Pedersen, T.: Geochemistry of recent oxic and anoxic marine sediments: Implications for the geological record, Mar Geol, 113, 67-88, 1993.

Calvert, S. and Pedersen, T.: Sedimentary geochemistry of manganese; implications for the environment of formation of manganiferous black shales, Econ Geol, 91, 36-47, 1996.

Carman, R. and Rahm, L.: Early diagenesis and chemical characteristics of interstitial water and sediments in the deep deposition bottoms of the Baltic proper, J Sea Res, 37, 25-47, 1997.

Carstensen, J., Andersen, J. H., Gustafsson, B. G., and Conley, D. J.: Deoxygenation of the Baltic Sea during the last century, PNAS 111, 5628-5633, 2014.

Conley, D. J., Björck, S., Bonsdorff, E., Carstensen, J., Destouni, G., Gustafsson, B. G., Hietanen, S., Kortekaas, M., Kuosa, H., Meier, H. E., Müller-Karulis, B., Nordberg, K., Norkko, A., Nürnberg, G., Pitkänen, H., Rabalais, N. N., Rosenberg, R., Savchuk, O. P.,

Slomp, C. P., Voss, M., Wulff, F., and Zillen, L.: Hypoxia-related processes in the Baltic Sea, Environ Sci Technol, 43, 3412-3420, 2009.

Dellwig, O., Leipe, T., März, C., Glockzin, M., Pollehne, F., Schnetger, B., Yakushev, E. V., Böttcher, M. E., and Brumsack, H.-J.: A new particulate Mn–Fe–P-shuttle at the redoxcline of anoxic basins, Geochim Cosmochim Acta, 74, 7100-7115, 2010.

Emerson, S., Jacobs, L., and Tebo, B.: The Behavior of Trace Metals in Marine Anoxic Waters: Solubilities at the Oxygen-Hydrogen Sulfide Interface. In: Trace Metals in Sea Water, Wong, C. S., Boyle, E., Bruland, K., Burton, J. D., and Goldberg, E. (Eds.), NATO Conference Series, Springer US, 1983.

Expedition 347 Scientists: Baltic Sea Basin Paleoenvironment: paleoenvironmental evolution of the Baltic Sea Basin through the last glacial cycle. *IODP Prel. Rept.*, 347, 2014. doi:10.2204/iodp.pr.347.2014

Feistel, R., Nausch, G., Mohrholz, V., Lysiak-Pastuszak, E., Seifert, T., Matthaus, W., Kruger, S., and Hansen, I. S.: Warm waters of summer 2002 in the deep Baltic Proper, Oceanologia, 45, 571-592, 2003.

Fennel, W.: A model of the yearly cycle of nutrients and plankton in the Baltic Sea, J Mar Syst, 6, 313-329, 1995.

Fonselius, S. and Valderrama, J.: One hundred years of hydrographic measurements in the Baltic Sea, J Sea Res, 49, 229-241, 2003.

Gustafsson, B. G. and Medina, M. R.: Validation data set compiled from Baltic Environmental Database. Version 2: Stockholm University Baltic Nest Institute Technical Report 2, 25 p., 2011.

Gustafsson, B. G., Schenk, F., Blenckner, T., Eilola, K., Meier, H. M., Müller-Karulis, B., Neumann, T., Ruoho-Airola, T., Savchuk, O. P., and Zorita, E.: Reconstructing the development of Baltic Sea eutrophication 1850–2006, Ambio, 41, 534-548, 2012.

Heiser, U., Neumann, T., Scholten, J., and Stüben, D.: Recycling of manganese from anoxic sediments in stagnant basins by seawater inflow: A study of surface sediments from the Gotland Basin, Baltic Sea, Mar Geol, 177, 151-166, 2001.

Hille, S., Nausch, G., and Leipe, T.: Sedimentary deposition and reflux of phosphorus (P) in the Eastern Gotland Basin and their coupling with P concentrations in the water column, Oceanologia, 47, 663-679, 2005.

Huckriede, H. and Meischner, D.: Origin and environment of manganese-rich sediments within black-shale basins, Geochim Cosmochim Acta, 60, 1399-1413, 1996.

Jakobsen, R. and Postma, D.: Formation and solid solution behavior of Ca-rhodochrosites in marine muds of the Baltic deeps, Geochim Cosmochim Acta, 53, 2639-2648, 1989.

Jilbert, T. and Slomp, C. P.: Iron and manganese shuttles control the formation of authigenic phosphorus minerals in the euxinic basins of the Baltic Sea, Geochim Cosmochim Acta, 107, 155-169, 2013.

Jilbert, T. and Slomp, C. P.: Rapid high-amplitude variability in Baltic Sea hypoxia during the Holocene, Geology, doi: 10.1130/g34804.1, 2013.

Jilbert, T., Slomp, C. P., Gustafsson, B. G., and Boer, W.: Beyond the Fe-P-redox connection: preferential regeneration of phosphorus from organic matter as a key control on Baltic Sea nutrient cycles, Biogeosciences, 8, 1699-1720, 2011.

Jochum, K. P., Weis, U., Stoll, B., Kuzmin, D., Yang, Q., Raczek, I., Jacob, D. E., Stracke, A., Birbaum, K., and Frick, D. A.: Determination of reference values for NIST SRM 610–617 glasses following ISO guidelines, Geostand Geoanal Res, 35, 397-429, 2011.

Jones, C., Crowe, S. A., Sturm, A., Leslie, K., MacLean, L., Katsev, S., Henny, C., Fowle, D. A., and Canfield, D. E.: Biogeochemistry of manganese in ferruginous Lake Matano, Indonesia, Biogeosciences, 8, 2977-2991, 2011.

Katsikopoulos, D., Fernández-González, A. and Prieto, M.: Precipitation and mixing properties of the “disordered” (Mn,Ca)CO3 solid solution, Geochim Cosmochim Acta 73, 6147-6161, 2009.

Kulik, D. A., Kersten, M., Heiser, U. and Neumann, T.: Application of Gibbs Energy Minimization to Model Early-Diagenetic Solid-Solution Aqueous-Solution Equilibria Involving Authigenic Rhodochrosites in Anoxic Baltic Sea Sediments, Aquatic Geochemistry 6, 147-199, 2000.

Lenz, C., Behrends, T., Jilbert, T., Silveira, M., and Slomp, C. P.: Redox-dependent changes in manganese speciation in Baltic Sea sediments from the Holocene Thermal Maximum: An EXAFS, XANES and LA-ICP-MS study, Chem Geol, 370, 49-57, 2014.

Lepland, A. and Stevens, R. L.: Manganese authigenesis in the Landsort Deep, Baltic Sea, Mar Geol, 151, 1-25, 1998.

Luther, G. W., Rickard, D. T., Theberge, S., and Olroyd, A.: Determination of metal (bi) sulfide stability constants of Mn2+, Fe2+, Co2+, Ni2+, Cu2+, and Zn2+ by voltammetric methods, Environ Sci Technol, 30, 671-679, 1996.

Lyons, T. W. and Severmann, S.: A critical look at iron paleoredox proxies: New insights from modern euxinic marine basins, Geochim Cosmochim Acta, 70, 5698-5722, 2006.

MacDonald, R. W. and Gobeil, C.: Manganese sources and sinks in the Arctic Ocean with reference to periodic enrichments in basin sediments, Aquat Geochem, 18, 565-591, 2012.

Madison, A. S., Tebo, B. M., and Luther, G. W.: Simultaneous determination of soluble manganese (III), manganese (II) and total manganese in natural (pore) waters, Talanta, 84, 374-381, 2011.

Manheim, F. T.: A geochemical profile in the Baltic Sea, Geochim Cosmochim Acta, 25, 52-70, 1961.

Martin, J.-M. and Meybeck, M.: Elemental mass-balance of material carried by major world rivers, Mar Chem, 7, 173-206, 1979.

Matthäus, W. and Schinke, H.: The influence of river runoff on deep water conditions of the Baltic Sea, Hydrobiologia, 393, 1-10, 1999.

Matthäus, W., Nehring, D., Feistel, R., Nausch, G., Mohrholz, V., and Lass, H.-U.: The Inflow of Highly Saline Water into the Baltic Sea. In: State and Evolution of the Baltic Sea, 1952–2005, John Wiley & Sons, Inc., 2008.

Meister, P., Bernasconi, S. M., Aiello, I. W., Vasconcelos, C., and McKenzie, J. A.: Depth and controls of Ca-rhodochrosite precipitation in bioturbated sediments of the Eastern Equatorial Pacific, ODP Leg 201, Site 1226 and DSDP Leg 68, Site 503, Sedimentology, 56, 1552-1568, 2009.

Mercone, D., Thomson, J., Abu-Zied, R., Croudace, I., and Rohling, E.: High-resolution geochemical and micropalaeontological profiling of the most recent eastern Mediterranean sapropel, Mar Geol, 177, 25-44, 2001.

Mort, H. P., Slomp, C. P., Gustafsson, B. G., and Andersen, T. J.: Phosphorus recycling and burial in Baltic Sea sediments with contrasting redox conditions, Geochim Cosmochim Acta, 74, 1350-1362, 2010.

Mucci, A.: The behavior of mixed Ca–Mn carbonates in water and seawater: controls of manganese concentrations in marine porewaters, Aquat Geochem, 10, 139-169, 2004.

Neumann, T., Christiansen, C., Clasen, S., Emeis, K.-C., and Kunzendorf, H.: Geochemical records of salt-water inflows into the deep basins of the Baltic Sea, Cont Shelf Res, 17, 95-115, 1997.

Neumann, T., Heiser, U., Leosson, M. A., and Kersten, M.: Early diagenetic processes during Mn-carbonate formation: Evidence from the isotopic composition of authigenic Ca-rhodochrosites of the Baltic Sea, Geochim Cosmochim Acta, 66, 867-879, 2002.

Pakhomova, S. V., Hall, P. O., Kononets, M. Y., Rozanov, A. G., Tengberg, A., and Vershinin, A. V.: Fluxes of iron and manganese across the sediment–water interface under various redox conditions, Mar Chem, 107, 319-331, 2007.

Parkhurst, D. L. and Appelo, C.: User's guide to PHREEQC (Version 2): A computer program for speciation, batch-reaction, one-dimensional transport, and inverse geochemical calculations, US Geological Survey Water-Resources Investigations Report 99-4259, 312 pp., 1999.

Pohl, C. and Hennings, U.: The coupling of long-term trace metal trends to internal trace metal fluxes at the oxic–anoxic interface in the Gotland Basin (57° 19, 20′ N; 20° 03, 00′ E) Baltic Sea, J Mar Syst, 56, 207-225, 2005.

Rickard, D.: The solubility of FeS, Geochim Cosmochim Acta, 70, 5779-5789, 2006.

Riley, J. P.: The Spectrophotometric Determination of Ammonia in Natural Waters with Particular Reference to Sea-Water, Anal Chim Acta, 9, 575-589, 1953.

Savchuk, O. P., Wulff, F., Hille, S., Humborg, C., and Pollehne, F.: The Baltic Sea a century ago—a reconstruction from model simulations, verified by observations, J Mar Syst, 74, 485-494, 2008.

Scholz, F., McManus, J., and Sommer, S.: The manganese and iron shuttle in a modern euxinic basin and implications for molybdenum cycling at euxinic ocean margins, Chem Geol, 355, 56-68, 2013.

Slomp, C. P., Malschaert, J. F. P., Lohse, L., and Van Raaphorst, W.: Iron and manganese cycling in different sedimentary environments on the North Sea continental margin, Cont Shelf Res, 17, 1083-1117, 1997.

Sternbeck, J. and Sohlenius, G.: Authigenic sulfide and carbonate mineral formation in Holocene sediments of the Baltic Sea, Chem Geol, 135, 55-73, 1997.

Strickland, J. D. H. and Parsons, T. R.: A practical handbook of seawater analysis, Fisheries Research Board of Canada, Ottawa, Canada, 1972.

Suess, E.: Mineral phases formed in anoxic sediments by microbial decomposition of organic matter, Geochim Cosmochim Acta, 43, 339-352, 1979.

Sundby, B., Silverberg, N., and Chesselet, R.: Pathways of manganese in an open estuarine system, Geochim Cosmochim Acta, 45, 293-307, 1981.

Turnewitsch, R. and Pohl, C.: An estimate of the efficiency of the iron-and manganese-driven dissolved inorganic phosphorus trap at an oxic/euxinic water column redoxcline, Global Biogeochem Cycles, 24, GB4025, 2010.

Ulfsbo, A., Hulth, S., and Anderson, L. G.: pH and biogeochemical processes in the Gotland Basin of the Baltic Sea, Mar Chem, 127, 20-30, 2011.

Yakushev, E. V., Kuznetsov, I. S., Podymov, O. I., Burchard, H., Neumann, T., and Pollehne, F.: Modeling the influence of oxygenated inflows on the biogeochemical structure of the Gotland Sea, central Baltic Sea: Changes in the distribution of manganese, Comput Geosci, 37, 398-409, 2011.

Yeats, P., Sundby, B., and Bewers, J.: Manganese recycling in coastal waters, Mar Chem, 8, 43-55, 1979.

Ziegler, M., Jilbert, T., de Lange, G. J., Lourens, L. J., and Reichart, G. J.: Bromine counts from XRF scanning as an estimate of the marine organic carbon content of sediment cores, Geochem Geophy Geosy, 9, Q05009, 2008.

Zillén, L., Lenz, C., and Jilbert, T.: Stable lead (Pb) isotopes and concentrations – A useful independent dating tool for Baltic Sea sediments, Quat Geochronol, 8, 41-45, 2012.

Table 1. Characteristics of the 8 study sites in the Baltic Sea. Redox: bottom water redox conditions at the time of sampling. Pore water samples were obtained during every cruise and were similar between years at each station. Here, the most complete data sets for each station are presented. Negative O_2 values indicate the presence of H_2S assuming that 1 mol of H_2S is equivalent to 2 mol O_2. Average sedimentation rates for the last 30 years are based on ^{210}Pb dating.

Site name	**Location**	**Cruise**	**Position**	**Water depth (m)**	**Sedimentation Rate (cm yr^{-1})**	**Redox**	**Salinity**
Fladen	Fladen	R/V Skagerak Sept. 2007	57°11.57N 11°39.25E	82	1.0	oxic	34.2
LF1	Northern Gotland Basin	R/V Aranda May/June 2009	57°58.95N 21°16.84E	67	0.25	oxic	8.2
BY5	Bornholm Basin	R/V Skagerak Sept. 2007	55°15.16N 15°59.16E	89	0.23	O_2=0.09 mLL^{-1}	16.2
LF3	Eastern Gotland Basin	Sediment: R/V Aranda May/June 2009 Pore water: R/V Pelagia May 2011	57°59.50N 20°46.00E	95	0.50	O_2=-0.13 mLL^{-1}	10.1
LL19	Northern Gotland Basin	Sediment: R/V Aranda May/June 2009 Pore water: R/V Heincke July 2010	58°52.84N 20°18.65E	169	0.30	O_2=-0.89 mLL^{-1}	11.4
BY15	Gotland Deep	Sediment R/V Aranda May/June 2009 Pore water: R/V Heincke July 2010	57°19.20N 20°03.00E	238	0.27	O_2=-3.32 mLL^{-1}	12.5
F80	Fårö Deep	Sediment: R/V Aranda May/June 2009	58°00.00N 19°53.81E	191	0.55	O_2=-2.04 mLL^{-1}	12.0

		Pore water: R/V Heincke July 2010					
LD1	Landsort Deep	R/V Pelagia May 2011	58°37.47N 18°15.23E	416	0.77	anoxic and sulfidic	10.6

1

Table 2. Diffusive fluxes of Mn across the sediment-water interface at all 8 sites. For further details, see text.

Site	**Location**	**Year and cruise**	**Depth range cm**	**Diffusive Mn flux µmol m^{-2} d^{-1}**
LF1	Northern Gotland Basin	2009 R/V Aranda	BW-0.25	115
BY5	Bornholm Basin	2009 R/V Aranda	BW-0.5	236
LF3	Eastern Gotland Basin	2009 R/V Aranda	BW-1	0
LL19	Northern Gotland Basin	2009 R/V Aranda	BW-0.25	81
BY15	Gotland Deep	2009 R/V Aranda	BW-0.25	98
F80	Fårö Deep	2009 R/V Aranda	BW-0.25	84
LD1	Landsort Deep	2011R/V Pelagia	BW*-2.5	~220

* LD1 has no measured bottom water sample. Therefore, the flux was estimated using the bottom water value from the Landsort Deep site BY31 from Mort et al. 2010.

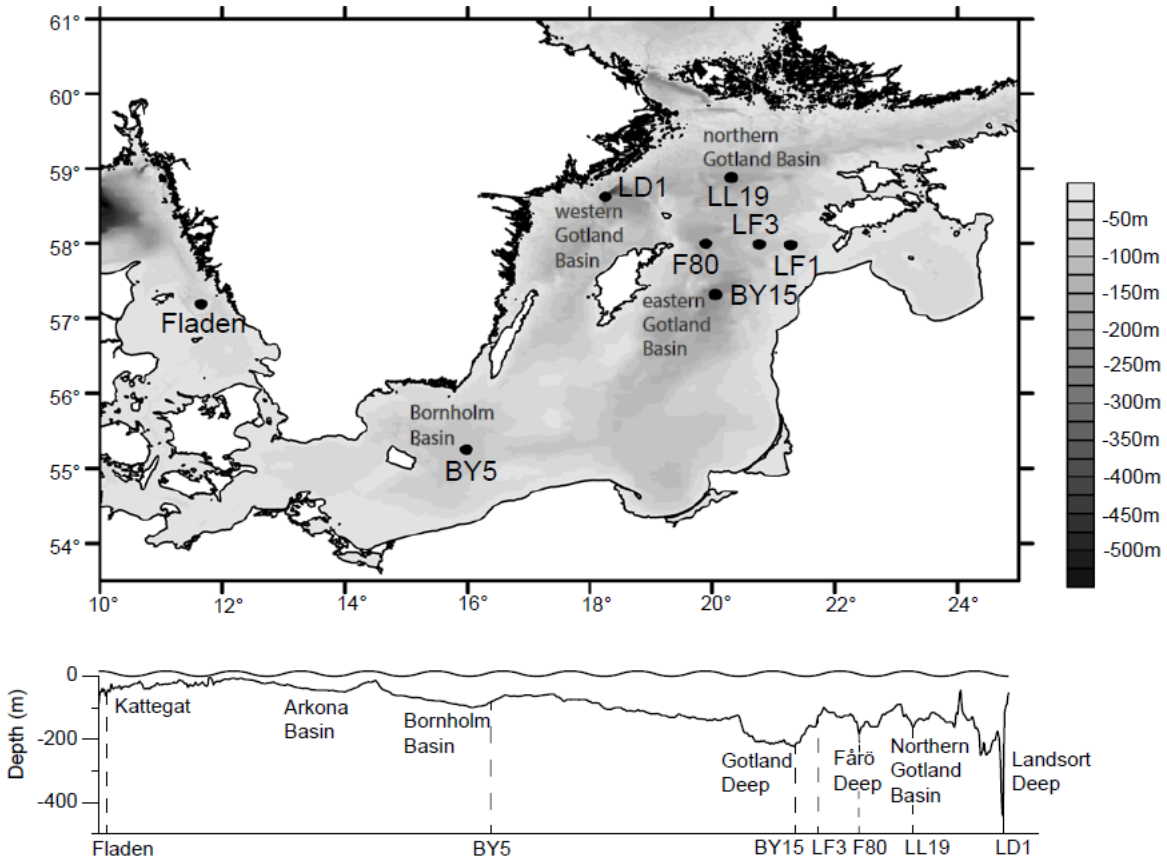

1

2 Figure 1 Bathymetric map and depth profile of the Baltic Sea showing the locations of the
3 sampling sites.

4

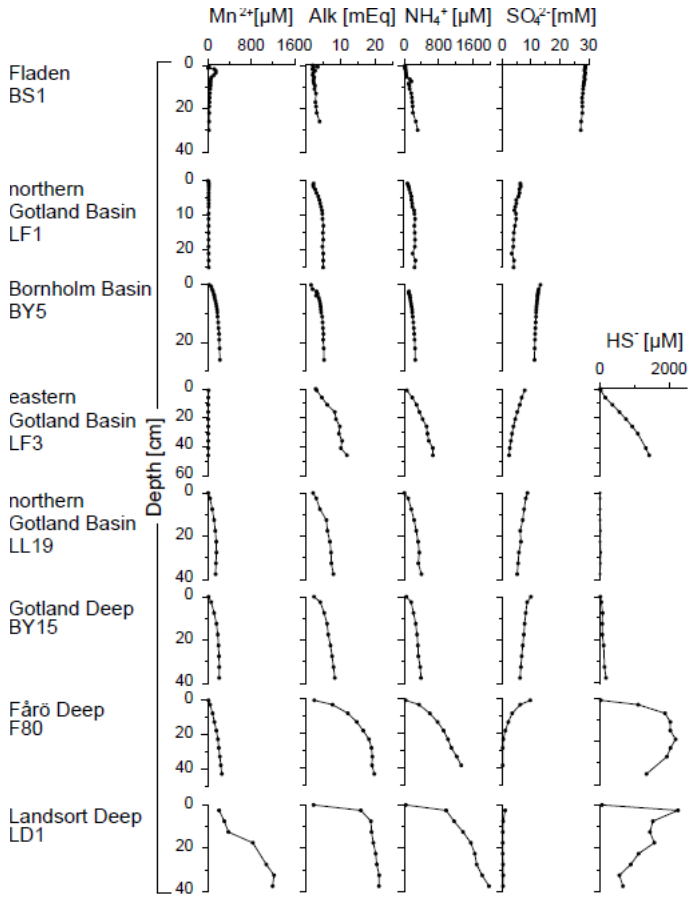

Figure 2 Pore water profiles of manganese (II), alkalinity, ammonium and sulfate for all 8 sites and hydrogen sulfide for the 5 deepest sites. Note, while dissolved sulfide is here expressed as HS^-, some H_2S is present as well.

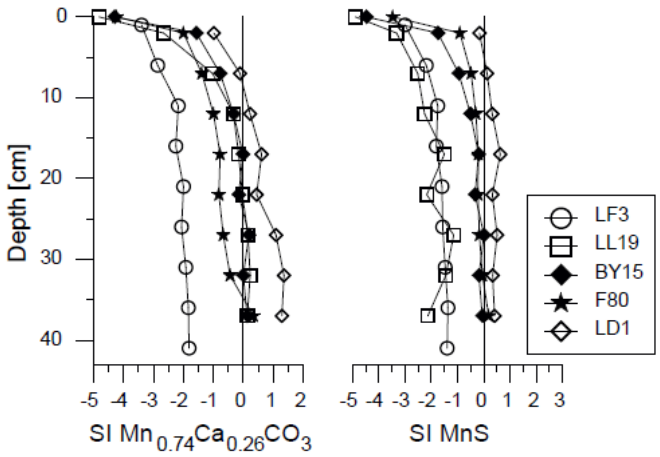

Figure 3 Saturation indices (SI) for $Mn_{0.74}Ca_{0.26}CO_3$ and MnS as calculated from the pore water data with PHREEQC.

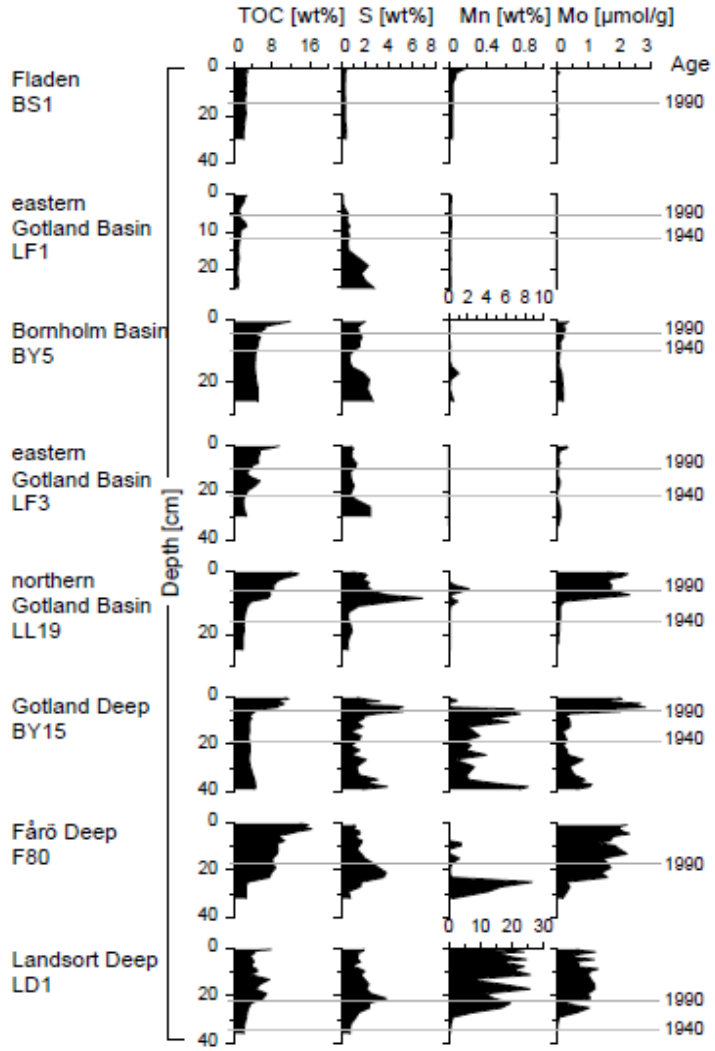

Figure 4 Sediment depth profiles of total organic carbon (TOC), sulfur (S), manganese (Mn) and molybdenum for all 8 sites. Note the different scale for manganese at Fladen and LF1, and LD1. Grey lines indicate the years 1990 and 1940, based on sediment dating. These date markers are used to demonstrate the variability of sedimentation rates in the study area.

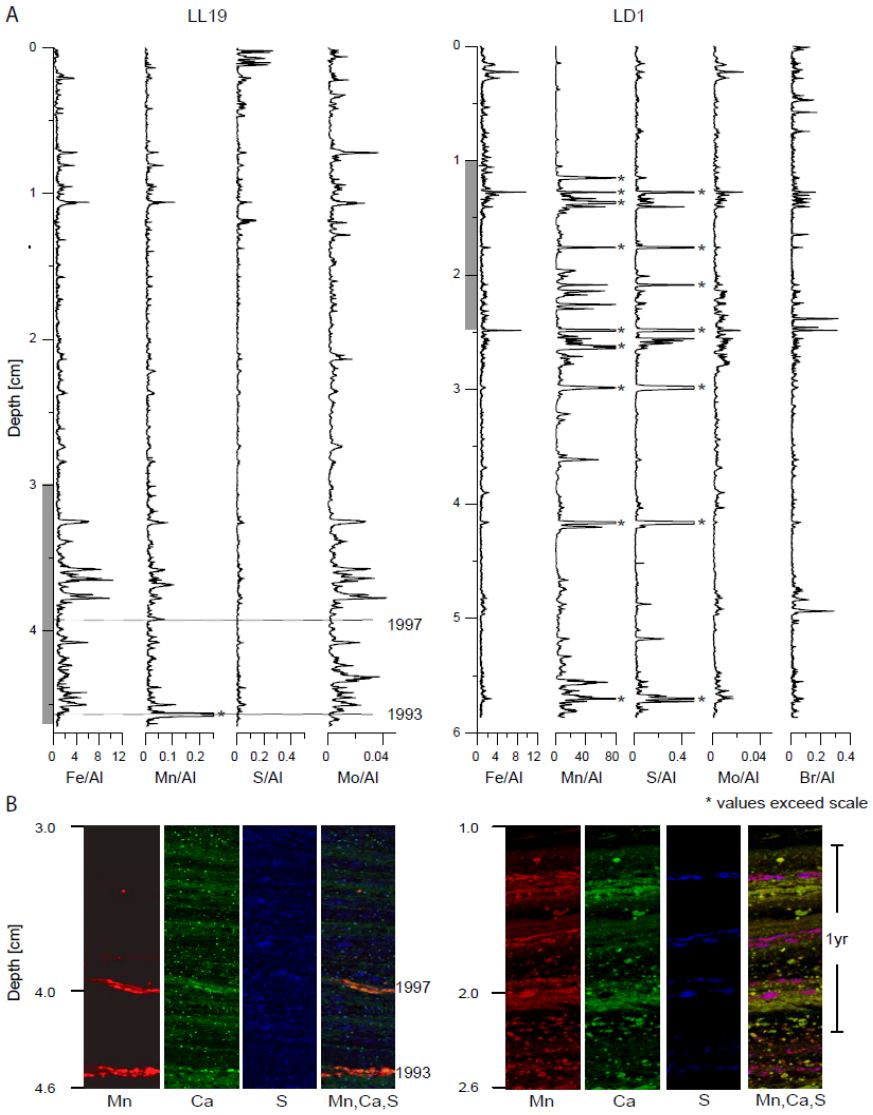

Figure 5 A: High resolution elemental profiles of Fe/Al, Mn/Al, S/Al, Mo/Al and Br/Al (only LD1) generated by LA-ICP-MS line scanning for resin-embedded surface sediment blocks. Note the difference in absolute values for Mn/Al between LL19 and LD1. The depth scale refers to the compacted sediment in the resin blocks (the total length of wet sediment prior to embedding was 5.5 cm (LL19) and 11.3 cm (LD1)). Peaks marked with a * exceed the scale. B: Compilation of micro XRF maps for station LL19 and LD1 showing the distribution of manganese (red), calcium (green) and sulfur (blue) at the depth indicated by grey panels in the LA-ICP-MS line scans. Color intensity within each map is internally proportional to XRF counts, but relative scaling has been modified to highlight features. The fourth picture for each station shows a RGB (red-green-blue) composite of the three elements with orange to yellow colors indicating a mix of Mn and Ca, and therefore, representing Ca-Mn carbonates. The pink/purple represents a mix of Mn and S, hence Mn sulfide.

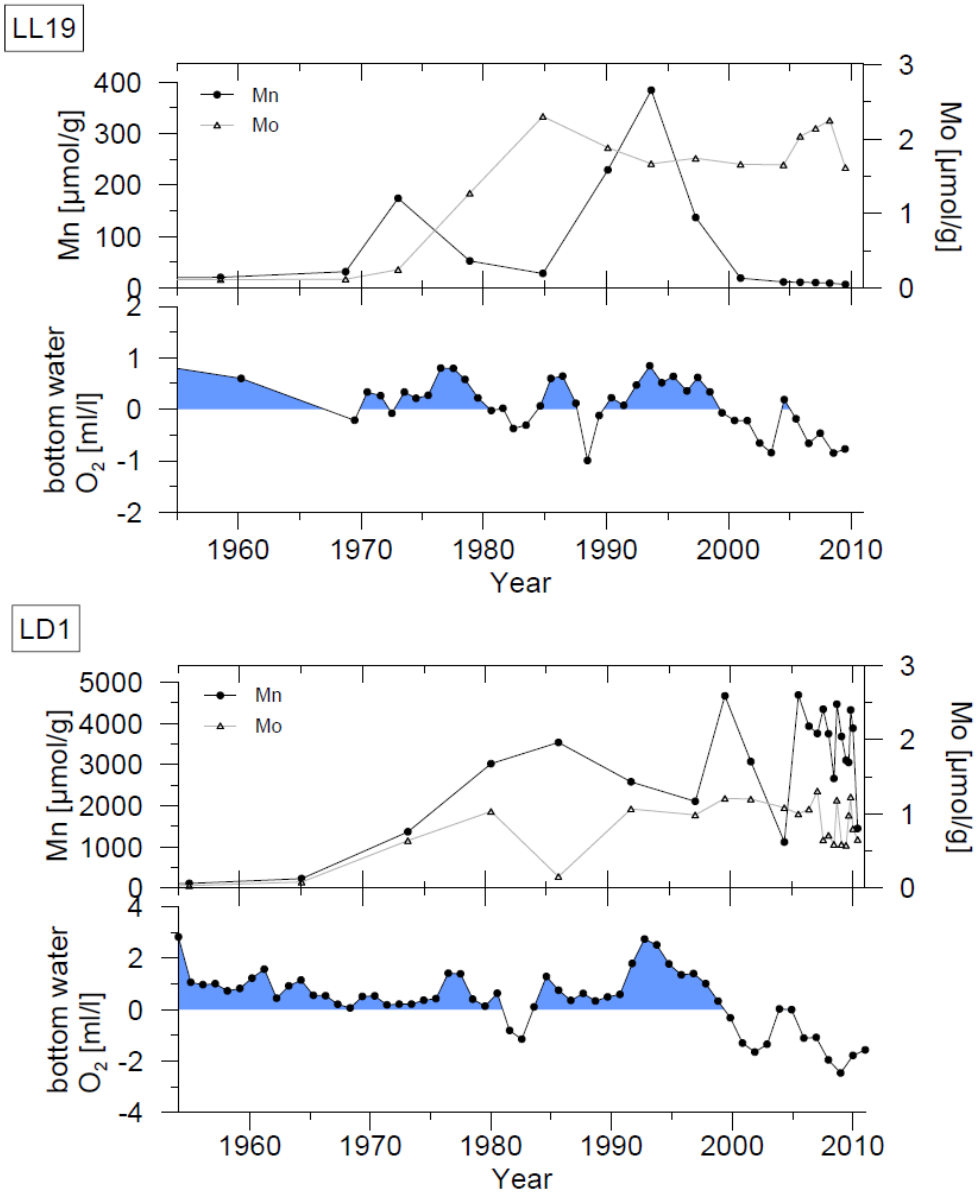

Figure 6 Records of sediment manganese and molybdenum for 1955-2010 for core LL19 and core LD1 and corresponding bottom water oxygen (Baltic Sea Environmental Database at Stockholm University; http://nest.su.se/bed/ACKNOWLE.shtml). Negative O_2 values indicate the presence of H_2S assuming that 1 mol H_2S is equivalent to 2 mol O_2.